Intercomparison between the NIST LBIR Absolute Cryogenic Radiometer and an Optical Trap Detector

S. R. Lorentz and R. U. Datla

Abstract. The goal of the Low Background Infrared (LBIR) calibration facility at the NIST is to provide the infrared user community with a measurement base for both broadband and spectral radiometric calibrations in a low background environment. The standard detector used in this facility is the Absolute Cryogenic Radiometer (ACR). The ACR is an electrical substitution radiometer which is capable of measuring between 20 nW and 100 μW of radiant power. By using an optical trap detector, an intercomparison with the ACR is made as part of a programme to monitor the long-term stability of the ACR. A comparison is also made between the optical trap detector and an in-house trap detector that was calibrated using the High Accuracy Cryogenic Radiometer (HACR).

1. Introduction

The Low Background Infrared Calibration Facility (LBIR) was initiated at the National Institute of Standards and Technology in 1989. The purpose of the facility is to provide the infrared user community with a measurement base for both broadband and spectral radiometric calibrations in a low background environment. Calibrations are carried out within a cryogenic vacuum chamber. The chamber is 60 cm in diameter and 1,6 m in length. The space allocated inside the chamber to house a user's source for calibration is a cubic volume of approximately 30 cm each side. Inside the chamber is a double-layer cryogenic shield. The outer shield is at a temperature of 40 K and the inner shield is at 20 K. The cryo-shields provide a low background environment in which to perform calibrations and experiments. Cooling for the chamber is provided by a closed-cycle helium refrigerator. In addition, the entire apparatus is enclosed in a soft-wall class 10000 clean room to insure cleanliness for optical measurements and users' sources. The facility currently provides broadband radiance calibrations for cryogenic black bodies and other sources employed in low background applications.

S. R. Lorentz and R. U. Datla: Radiometric Physics Division, National Institute of Standards and Technology, Gaithersburg, MD 20899, USA.

2. Description of the ACR

The standard detector used in the LBIR facility is the Absolute Cryogenic Radiometer (ACR). The radiometer was manufactured for the facility by Cambridge Research and Instrumentation, Inc. (CRI) [1]. The ACR, shown as an outline drawing in Figure 1, is an

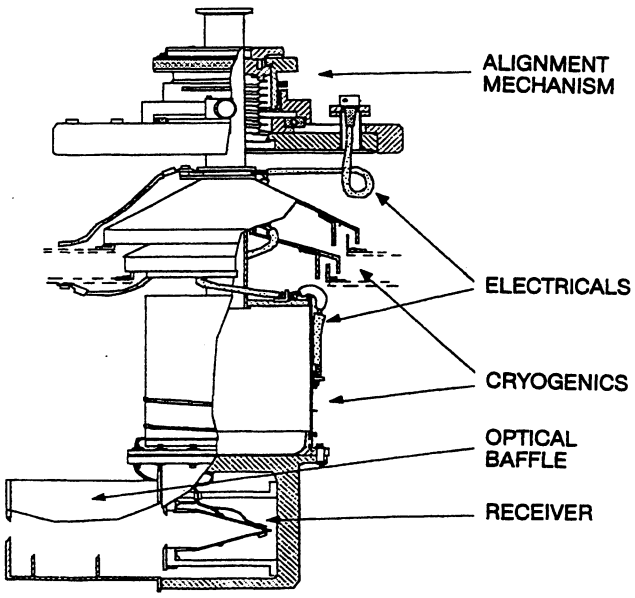

Figure 1. Diagram of the Absolute Cryogenic Radiometer.

electrical substitution radiometer capable of measuring radiant flux levels between 20 nW and 100 μW. The ACR is mounted on a 30 cm diameter ultrahigh vacuum flange. Cryogenic operation is provided by a 3 litre liquid helium cryostat that is pressure controlled to lower the operating temperature of the ACR to 2,2 K. The temperature of the receiver cone is measured by two germanium resistance thermometers. The responsivity of the radiometer is 29,7 K/mW at an operating temperature of 2,2 K. The natural time constant associated with the receiver cone is approximately 20 seconds. The radiometer can be moved between three different ports in the vacuum chamber, thereby changing the distance between the source and the radiometer to 30 cm, 63 cm, or 96 cm. A more complete discussion of the ACR and its characterization can be found in an earlier publication [2].

The electronics that provide computer control of the ACR and perform the electrical substitution measurements were recently upgraded to a new design

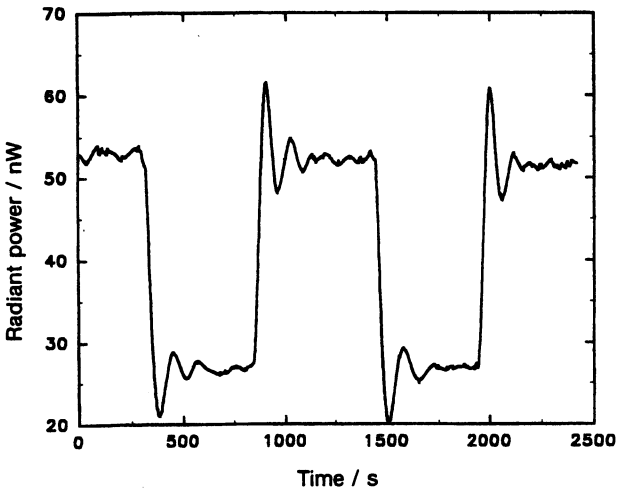

Figure 2. Receiver power as a function of time measured with the original electronics.

by CRI. Figure 2 shows a plot of sample data taken with the ACR using the previous version of the electronics. The plot shows the temporal response of the ACR to opening and closing a shutter on a source generating 25 nW of radiant power. The noise on the signal is of order ±0,5 nW. A plot of sample data taken with the revised electronics is shown in Figure 3. The power measured is approximately 6 nW; note that the noise level is down significantly from that in Figure 2 and is now approximately ±0,1 nW. The new electronics are employed in the intercomparisons presented later in the paper. The uncertainties associated with the ACR and shown in Table 1 are described in [2]. The combined standard uncertainty given as the sum in quadrature of the individual components is equal to 0,12 %. All uncertainties in this paper are given at the level of one standard deviation.

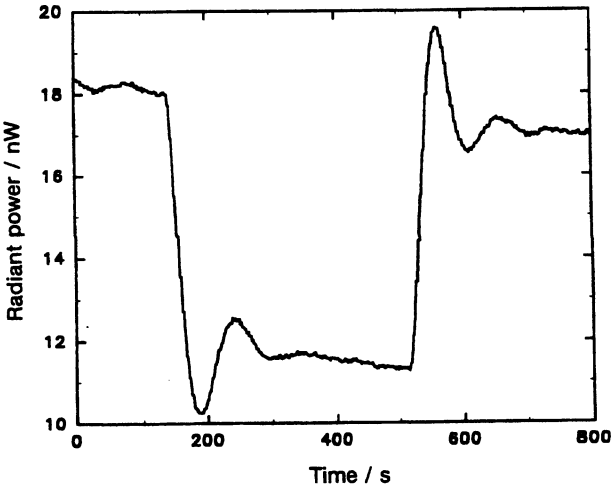

Figure 3. Receiver power as a function of time measured with the updated electronics.

Table 1. Uncertainties associated with the ACR.

Current sense resistor	0,01 %
Electrical power measurement	0,05 %
Heater nonequivalence	0,03 %
Receiver absorptance	0,10 %

3. Intercomparison between the ACR and an Optical Trap Detector

Characterization of the ACR is an integral part of the calibration process. A comparison with different absolute detectors is performed as part of that characterization. An intercomparison has been carried out between the ACR and a United Detector Technology QED-200 which is an absolute radiometric standard for use between 360 nm and 800 nm. This detector has an uncertainty of 0,1 % over this wavelength range. The QED-200 consists of three silicon photodiodes mounted in a trap configuration. The photodiodes are arranged such that the first two are at 45° with respect to the incident flux and the second is also rotated 90° with respect to the first detector. The third is set normal to the incident flux, thereby reflecting the light back to the first two detectors. These silicon photodiodes have an internal quantum efficiency very near 100 %; however, the surface of the detector is not perfectly absorbing. The detectors are arranged in this trap configuration to provide for a total of five opportunities for collection of the light by absorption. The rotation of the second detector with respect to the first aids in eliminating the polarization sensitivity of the detector. The responsivity I of the silicon photodiodes over the useful spectral range [3] is given by

$$R=[(\lambda/\mathrm{nm})/1\,239{,}5]\,\mathrm{AW}^{-1}, \quad (1)$$

where λ is the wavelength of the incident light.

The experimental arrangement for the intercomparison of the QED-200 with the ACR is shown in

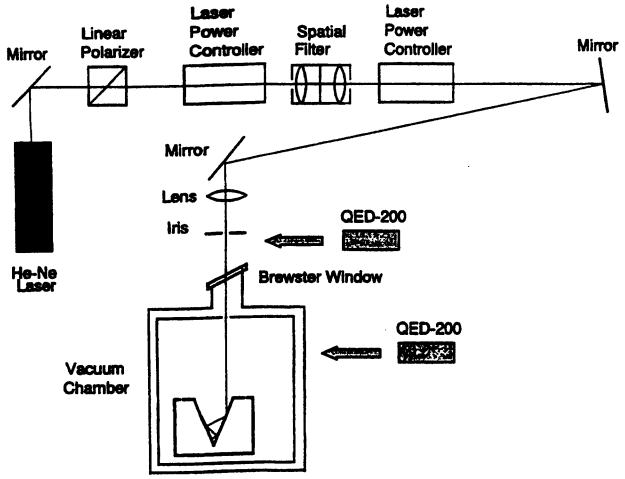

Figure 4. Experimental arrangement for the QED-200 versus ACR comparison.

Figure 4. A 633 nm He-Ne laser was used as the light source for this work. The radiation was linearly polarized with a Glan-Thomson polarizer. A commercial power controller was used to stabilize the laser power. This provided a stabilized light source with a specified typical drift in laser power of 0,05 % over an eight hour period. The beam was passed through a spatial filter to reduce scattered light along the path of the beam. A lens placed outside the vacuum chamber was used to focus the beam to a spot size of 3 mm at the receiver cone of the ACR. The Brewster window was a fused silica glass set at an angle of 57° to the incident beam and aligned to transmit vertically polarized light into the vacuum system. Nonlimiting apertures were used at the inner and outer cryogenic shields and in front of the ACR receiver cone in order to reduce the ambient background flux levels. This was required since the ACR is sensitive to wavelengths of over 100 μm. The background flux level measured with the ACR was found to be approximately 1 μW, a small fraction of the typical signal level of 60 μW. The background flux is removed from the experiment by taking measurements with the laser beam on, followed by a measurement where the laser beam is shuttered. The difference between the two measurements is then taken to be a measurement of the power in the laser beam.

The ACR must be operated in a cryogenic vacuum, but the QED-200 was designed to be operated at ambient temperatures and pressures. The intercomparison therefore had to be made with the QED-200 outside the vacuum chamber at room temperature, and the window through which the ACR was illuminated had to be characterized to account for any losses. The first step in the experiment was to characterize the transmission of the silica window so that its effect could be removed from the comparison between the QED-200 and the ACR. The QED-200 was used to measure the laser power both inside and outside the chamber at the positions indicated in Figure 4. Possible changes in the transmission due to stress when the window is under vacuum were not taken into account. This proved to be a negligible effect relative to other factors in the error budget for the intercomparison. The photoresponse current I from the QED-200 is related to the power in the laser beam P_{QED} by

$$P_{QED} = I/R$$

and

$$R = (632{,}8/1\,239{,}5)\,\mathrm{AW}^{-1}. \qquad (2)$$

This measurement was conducted at ambient temperature and pressure with the QED-200 moved alternately from inside to outside the chamber. The laser power controller was set to produce approximately 60 μW of power at the ACR receiver cone. The window transmission T_{win} was measured to be $0{,}996\,41 \pm 0{,}000\,43$.

In order to operate the ACR, the vacuum chamber was sealed and evacuated, then cooled to 20 K. After the ACR was cooled to its operating temperature of approximately 2,2 K, the next stage in the comparison was carried out. The QED-200 was inserted into the laser beam at its outside position. After a measurement was made, the QED-200 was removed from the optical path so that the beam could be measured using the ACR. This interchange of detectors was carried out repeatedly for laser powers of 30 μW, 60 μW and 90 μW. The results of this experiment are listed in Table 2; the uncertainties expressed

Table 2. Ratio of the laser power as measured by the QED-200 versus the ACR.

$P_{ACR}/\mu W$	$R_{QED/ACR}$
31,00	$1{,}000\,2 \pm 0{,}000\,4$
62,07	$1{,}000\,4 \pm 0{,}000\,4$
92,96	$1{,}000\,4 \pm 0{,}000\,4$

are those arising from random effects. The laser power P_{ACR} is the value of the power measured by the ACR divided by T_{win} to correct for the window transmission. The ratio $R_{QED/ACR}$ is defined as P_{QED}, the power measured by the QED-200, divided by P_{ACR},

$$R_{QED/ACR} = P_{QED}/P_{ACR}. \qquad (3)$$

The intercomparison shown in Table 2 demonstrates that the ACR is in agreement with the QED-200 to within 0,04 % at 633 nm. Future work will extend such comparisons into the infrared.

The results show that the ACR, as an absolute detector, compares well with the QED-200 optical trap detector. Two years ago a similar comparison was made between the ACR and a QED-200 [2]. The present measurements were made with smaller uncertainties and show a better agreement between the ACR and the QED-200. The ACR has shown no degradation during the past two years of operation.

4. Intercomparison between the ACR and the HACR

Having completed an intercomparison between the ACR and a QED-200, we then compared the absolute scale of the ACR with that of the High Accuracy Cryogenic Radiometer (HACR). The HACR is an absolute detector used in the Radiometric Physics Division at the NIST to calibrate transfer detectors at laser wavelengths [4]. The calibration of an optical trap detector package produced in-house, called the HMT detector, has an uncertainty of 0,015 %. The HMT consists of three Hamamatsu silicon photodiode detectors arranged in a trap configuration with the outputs from the detectors summed together. A comparison was conducted, using 633 nm laser light, between the QED-200 detector and two different HMT detectors both of which had recently been calibrated using the HACR.

The measurements were carried out at a laser power level of approximately 90 μW with the experimental setup described in Figure 4. The laser power was measured by the QED-200 in its position outside the chamber, and then the laser beam was shuttered and a background measurement taken. One of the HMT detectors was then swapped into the position of the QED-200 and the measurement repeated. This cycle was carried out many times for the QED-200 and each of the two HMTs. The result for each HMT, as measured by the HACR for 633 nm, was used to calculate the power measured. The ratios of the results for each HMT and the QED-200 are shown in Table 3.

These data allow comparison of the absolute scales of the ACR and the HACR. The ratio of the measured laser powers from the QED-200 and the ACR give a result of $1{,}000\,4 \pm 0{,}000\,4$. The average of the results of the comparison of the QED-200 with the two HMTs is $1{,}000\,69 \pm 0{,}021$ %. The ACR scale can thus be related to the HACR scale by $1{,}000\,4 \times 1{,}000\,69 = 1{,}001\,1$. The uncertainties relating to this quantity are shown in Table 4. The combined standard relative uncertainty given as the sum in quadrature of the individual components is equal to 0,16 %.

Table 3. The ratios of the power measured by the HMTs to the QED-200.

HMT #1/QED-200
$(92{,}993 \pm 0{,}000\,11)/(92{,}914 \pm 0{,}000\,13) = 1{,}000\,85 \pm 0{,}000\,15$
HMT #2/QED-200
$(92{,}962 \pm 0{,}000\,11)/(92{,}914 \pm 0{,}000\,13) = 1{,}000\,51 \pm 0{,}000\,15$

Table 4. Uncertainties in the comparison of the ACR with the HACR.

Combined uncertainty of the calibration of the HMTs	0,015 %
Systematic uncertainty in the ratio of the QED-200 to the ACR	0,120 %
Systematic uncertainty in the responsivity of the QED-200	0,100 %
Random uncertainty in the HMT to QED ratio	0,021 %

5. Conclusions

Intercomparisons of absolute detectors and of checking calibration procedures are essential to the maintenance of an absolute radiometric base. The comparisons presented here demonstrate that the ACR compares well with the HACR within its estimated uncertainties, resulting in excellent agreement between two very different cryogenic radiometers. Future comparisons will be made with improved accuracy.

Note. The identification within this paper of particular commercial equipment does not imply recommendation or endorsement by the National Institute of Standards and Technology, but is done to more accurately describe the experimental procedure.

References

1. Hoyt C. C., Foukal P. V., *Metrologia*, 1991, **28**, 163-167.
2. Datla R. U., Stock K., Parr A. C., Hoyt C. C., Miller P. J., Foukal P. V., *Appl. Opt.*, 1992, **31**, 7219-7225.
3. Zalewski E. F., Duda C. R., *Appl. Opt.*, 1983, **22**, 2867-2873.
4. Houston J. M., Cromer C. L., Hardis J. E., Larason T. C., *Metrologia*, 1993, **30**, 285-290.